

Design of an Alternative Coolant Inlet Flow Configuration for the Modular Helium Reactor

**International Congress on Advances in
Nuclear Power Plants (ICAPP 06)**

S.M. Mohsin Reza
Edwin A. Harvego
Matt Richards
Arkal Shenoy
Kenneth Lee Peddicord

June 2006

The INL is a
U.S. Department of Energy
National Laboratory
operated by
Battelle Energy Alliance



This is a preprint of a paper intended for publication in a journal or proceedings. Since changes may be made before publication, this preprint should not be cited or reproduced without permission of the author. This document was prepared as an account of work sponsored by an agency of the United States Government. Neither the United States Government nor any agency thereof, or any of their employees, makes any warranty, expressed or implied, or assumes any legal liability or responsibility for any third party's use, or the results of such use, of any information, apparatus, product or process disclosed in this report, or represents that its use by such third party would not infringe privately owned rights. The views expressed in this paper are not necessarily those of the United States Government or the sponsoring agency.

Design of an Alternative Coolant Inlet Flow Configuration for the Modular Helium Reactor

SM Mohsin Reza

Texas A&M University, College Station, TX 77843-3133,
Tel. (979) 845-4100, Fax. (979) 845 6443, Email: mreza@ne.tamu.edu

Edwin A Harvego

Idaho National Laboratory, PO Box 1625, Idaho Falls, ID 83415-3885
Tel: (208) 526 954, Email: Edwin.Harvego@inl.gov

Matt Richards

General Atomics, P.O Box 85608, San Diego, CA 92186-5608
Tel: (858) 455-2457, Fax: (858) 455-2599, Email: matt.richards@gat.com

Arkal Shenoy

General Atomics, P.O Box 85608, San Diego, CA 92186-5608
Tel. (858) 455-2552, Fax. (858) 455-2469, Email: Arkal.Shenoy@gat.com

Kenneth Lee Peddicord

Texas A&M University, College Station, TX 77843-3133,
Tel. (979) 458-6010, Fax. (979) 845 6443, Email: k-peddicord@tamu.edu

Abstract - The coolant outlet temperature for the Modular Helium Reactor (MHR) was increased to improve the overall efficiency of nuclear hydrogen production using either thermochemical or high temperature electrolysis (HTE) processes. The inlet temperature was also increased to keep about the same ΔT across the reactor core. Thermal hydraulic analyses of the current MHR design were performed with these updated temperatures to determine the impact of these higher temperatures on pressure drops, coolant flow rates, and temperature profiles within the vessel and core regions. Due to these increased operating temperatures, the overall efficiency of hydrogen production processes increases but the steady state reactor vessel temperature is found to be well above the ASME code limits for current vessel materials.

Using the RELAP5-3D/ATHENA computer code, an alternative configuration for the MHR coolant inlet flow path was evaluated in an attempt to reduce the reactor vessel temperatures. The coolant inlet flow was shifted from channel boxes located in the annular region between the reactor core barrel and the inner wall of the reactor vessel to a flow path through the outer permanent reflector. Considering the available thickness of graphite in the permanent outer reflector, the total flow area, the number of coolant holes, and the coolant-hole diameter were varied to optimize the pressure drop, the coolant inlet velocity, and the percentage of graphite removed from the core. The resulting thermal hydraulic analyses of the optimized design showed that peak vessel and fuel temperatures were within acceptable design limits for both steady-state and transient operating conditions.

I. INTRODUCTION

The steady state reactor vessel temperature is one of the biggest concerns still to be addressed to accomplish the design of MHR for high efficiency nuclear hydrogen production. The high temperature capability and advance stage of development of the MHR make it a strong candidate for nuclear hydrogen production using either the Sulfur-Iodine (SI) based thermochemical process or High Temperature Electrolysis (HTE) process¹. However, the temperatures required for efficient hydrogen production

(900 °C – 1000 °C) present a unique design challenge for the reactor pressure vessel during steady-state operation. As part of a Nuclear Energy Research Initiative (NERI) project sponsored by the United States Department of Energy (DOE), an investigation of an alternative vessel inlet coolant flow scheme was undertaken in an attempt to achieve lower reactor vessel temperatures during steady-state operation.

The NERI project was led by General Atomics (GA) and supported by the Idaho National Laboratory (INL), Texas A&M University and Entergy Nuclear, Inc.

The results of thermal-hydraulic analyses of an alternative coolant inlet configuration for the MHR, that allows higher reactor vessel outlet temperatures while maintaining acceptable steady-state reactor vessel wall temperatures is the subject of this paper. The new coolant inlet flow configuration described in this paper, is through the permanent outer reflector, also referred as permanent side reflector (PSR). During this study, alternative flow path geometries were evaluated while maintaining the total pressure drop, the amount of graphite removal from the core (to create the coolant flow passages), and the inlet coolant velocity within acceptable limits.

II. MHR SYSTEM

The design of MHR for hydrogen production applications based on the Gas Turbine-Modular Helium Reactor (GT-MHR) is developed by GA. Fig. 1 shows the reactor system. This passively safe reactor is helium cooled and graphite moderated, with a power density as low as $\sim 6.5 \text{ w/cm}^3$.

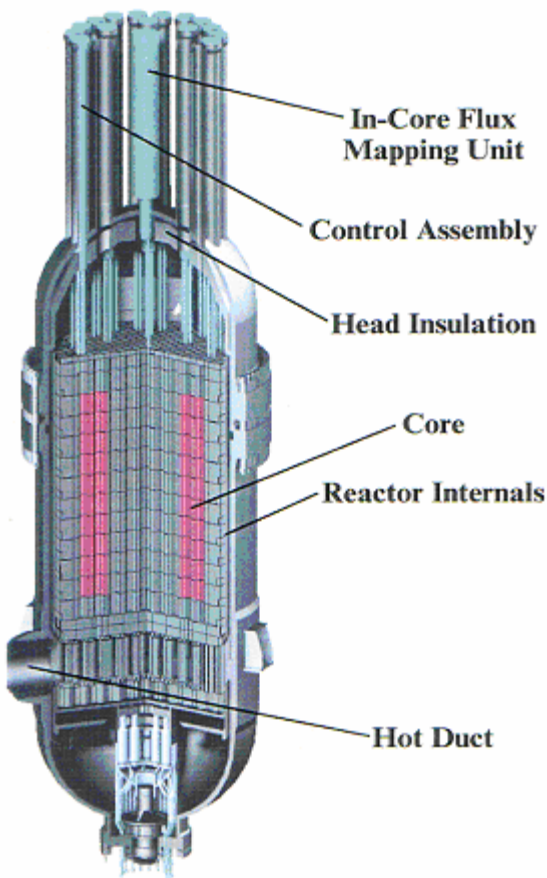


Fig. 1. MHR system

The prismatic reactor core consists of hexagonal graphite blocks. The annular fuel region is surrounded by inner and outer reflectors. About one third of the total blocks are fuel blocks and remaining two thirds are reflector blocks. During transients the large amount of graphite acts as a temporal heat sink to keep the peak fuel temperature well below the design temperature limit. The high volumetric heat capacity of the nuclear grade graphite also ensures long delay before the fuel attains its peak temperature during transient or upset conditions.

The passive safety of this reactor system is accomplished by conducting decay heat radially through the core and pressure vessel and transferring the heat by radiation and convection into a passive air-cooled reactor cavity cooling system (RCCS). The reactor also has a reserve shutdown control system, and a non-safety shutdown cooling system used only to remove decay heat during normal shutdowns. More detailed information on the MHR design is contained in a number of references²⁻⁴.

In the GT-MHR design, the inlet helium at 490°C and $\sim 7 \text{ MPa}$ flows upwards through the rectangular box-shaped flow paths located in the annulus between the reactor core barrel and the reactor vessel wall. The inlet helium temperature is the main determinant of vessel operating temperature. The helium then flows through the reactor core inlet plenum and downward through the core. The majority of the coolant flows through the coolant holes in the core. A fraction of the total flow ($\sim 10\%$) bypasses these core coolant channels, passing through the gaps between the fuel elements and reflector blocks.

III. NEW COOLANT CONFIGURATION

To accommodate the higher temperatures required for hydrogen production, the coolant inlet and outlet temperatures of 490°C and 850°C in the original MHR design were increased to 590°C and 950°C , respectively. This increase in reactor temperatures results in an increase in overall hydrogen production efficiency for both the SI and HTE based hydrogen production processes from about 40% at 850°C to about 50% at 950°C ^{5,6} while maintaining about the same coolant flow and convective heat transfer rates within the core. Coolant outlet temperatures beyond this would further increase the hydrogen production efficiency, but it was limited to 950°C to avoid any potential adverse impacts on fuel performance during normal steady state operation of the MHR⁷. In addition, a coolant outlet temperature beyond 950°C would create a significant design challenges for the intermediate heat exchanger that transfer heat from the primary system through an intermediate loop to the hydrogen production process.

Initial calculations for the current GT-MHR coolant flow configuration with the vessel inlet and outlet helium temperatures increased to 590°C and 950°C

respectively, produced a peak steady state reactor vessel temperature of about 541 °C, which is well above the ASME code limit for current reactor vessel material. In an attempt to reduce the steady state reactor vessel temperature, the coolant inlet flow path was shifted from the channel boxes located in the annular region between reactor vessel and the core barrel to new coolant flow holes through the permanent outer reflector. Fig. 2 shows the schematic of the flow path for both the old and the new coolant flows. The original coolant inlet flow through the channel boxes between the reactor core barrel and vessel wall is shown with cross (X) signs.

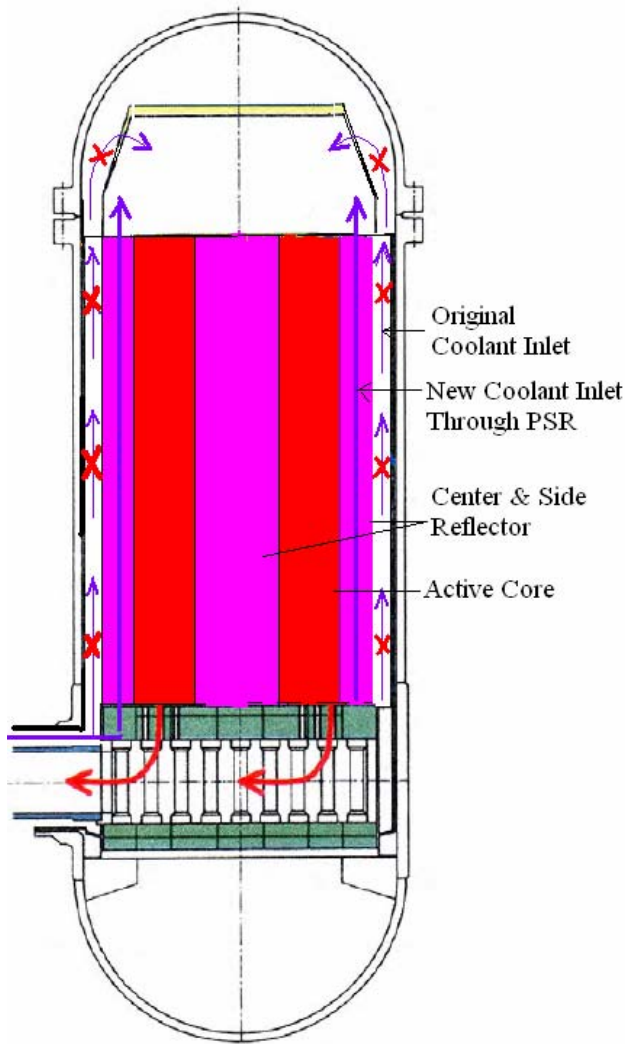


Fig. 2. The old and new coolant path through the MHR system

The development and evaluation of the new coolant flow path was done in several steps. In the first step the pressure drop, coolant inlet velocity and amount of graphite removed to create the inlet flow path, were optimized. Based on this optimization and the available thickness of permanent outer reflector, the number of coolant inlet holes and their dimensions were selected (second step). In the third step, the relevant changes for the radiation and conduction heat transfer calculations in an existing MHR ATHENA model were made to account for the removal of graphite from reactor core and to calculate the exact heat transfer in the core during normal and transient operation

IV. ATHENA CALCULATION

The foundation of the ATHENA⁸ (Advanced Thermal Energy Network Analysis) computer code is the RELAP5-3D⁹ computer code, both of which were developed at the INL. To expand the capability of the RELAP code, new working fluids, new heat transfer models, and a magneto-hydrodynamic model were added to this code. The addition of new working fluids allows the ATHENA code to be used for advanced reactor designs including the MHR. In addition, the ATHENA code can also be used for space reactor applications since it can perform variable gravity calculations with user defined gravitational constants.

The original RELAP5-3D/ATHENA model of the MHR was developed at the INL. This is a simplified model that is designed to examine the core behavior. The model includes the reactor vessel shown in Fig. 3 and the reactor cavity cooling system (RCCS) shown in Fig. 4.

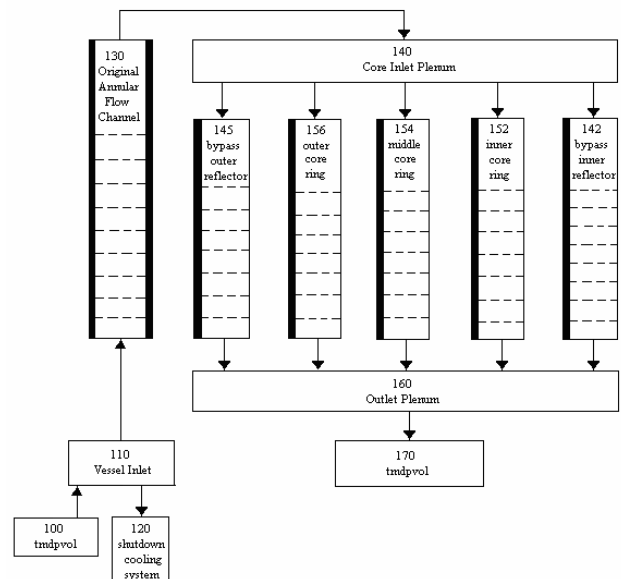


Fig. 3. The original reactor vessel nodalization

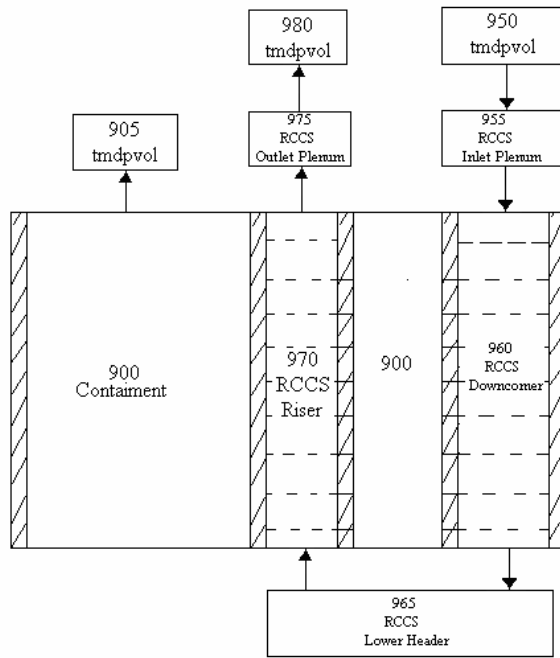


Fig. 4. Containment and RCCS nodalization for ATHENA model

Limited validation of this original ATHENA model was performed using available design data for the MHR. When a reasonable representation of the expected nominal steady state conditions was reproduced, this validation process was considered complete. In the case of the transient validation, the results of transient calculations such as Low Pressure Conduction Cooldown (LPCC) and High Pressure Conduction Cooldown (HPCC) were compared for consistency and reasonableness of results. The steady state validation, consisting of a comparison of several nominal steady state expected values and the ATHENA calculated values are shown in Table I. The transient validation results are shown in Table II.

TABLE I

MHR Design Value and Steady State Calculated Value

Parameters	Expected Value	ATHENA Calculation
Coolant flow rate (kg/s)	320	324.18
Core pressure drop (MPa)	0.051	0.0508
RCCS power (MW)	3.3	3.2926
RCCS flow rate (kg/s)	14.3	14.1481
RCCS air outlet temp. ($^{\circ}$ C)	274	270.757
Reactor vessel temperature ($^{\circ}$ C)	446	453

TABLE II

Result of MHR Transient Validation

Parameters	LPCC Transient pressure 1 atm.		HPCC Transient pressure 5.03 MPa.	
	Expected	ATHENA	Expected	ATHENA
Peak fuel temperature ($^{\circ}$ C)/time (h)	1447/63	1437/58.7	1223/45	1276/58
Peak Vessel temperature ($^{\circ}$ C)/time (h)	502/81	500/77.5	457/70	467/73.8

V. Modified ATHENA Model

Fig. 5 shows a modified reactor vessel nodalization including the new coolant configuration. The coolant enters the vessel at the vessel inlet (component 110). In the original ATHENA model, the coolant flow path was up through the channel boxes located in the annular region between reactor vessel and reactor core barrel (component 130) to the core inlet plenum (component 140). The inlet flow was assumed to occupy the entire region between the core barrel and the reactor vessel including the dead helium volume.

In the revised model, volume 132 represents the new coolant flow path through the permanent outer reflector. The outlet of this flow path enters directly into the core inlet plenum instead of flowing past the upper head and into the core inlet plenum through holes in the upper plenum shroud (as in the current design). Therefore, in the revised coolant flow configuration, the hot inlet helium does not transfer heat directly to the reactor vessel upper head. In addition, in this new design, the inlet plenum (component 110) is insulated to preclude heat transfer to the vessel wall in the lower core region. All these modifications were incorporated into the ATHENA model accordingly. Volume 130 is modeled as a stagnant volume connected to the outlet of the vessel inlet plenum, but with no direct connection to the core inlet plenum.

As shown in Fig. 5, coolant flows from the core inlet plenum down through the core. The core is modeled with three parallel channels (component 152, 154 and 156), each representing one of the three rings in the annular fueled region. Two core bypass channels are modeled; they are central reflector (component 142) and outer reflector (component 145). After passing through the core the coolant flows through the core outlet plenum (component 160) and finally flows out of the vessel. The inlet flow is controlled to achieve the desired helium outlet temperature and two time dependent volumes (component 100 and 170) provide the system boundary conditions.

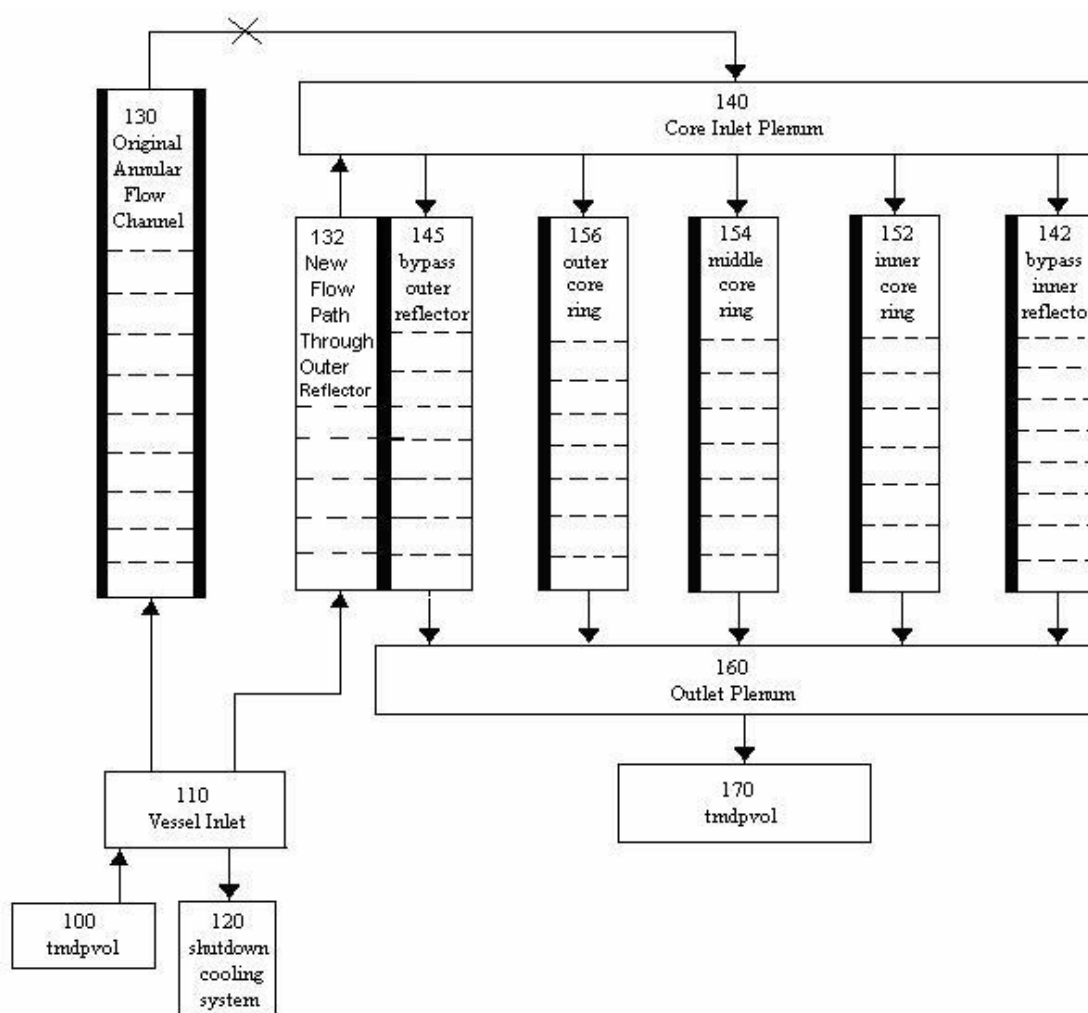


Fig. 5. Modified ATHENA-nodalization for MHR vessel

Heat structures are used to model most of the structural components in the vessel. The active core has ten axial nodes each representing one of the fuel blocks. The upper and the lower reflectors are also modeled as two additional axial blocks. The containment, including its surrounding wall and the RCCS which is located on the interior of the containment, are also modeled

Radial and axial conduction are modeled in the core and reflectors. Radiation heat transfer is modeled from the core barrel to the reactor vessel then to the RCCS, and finally to the containment wall. The RCCS is modeled as a dry air-filled system. The risers are modeled as three separate structures, connected by conduction.

The outer permanent and replaceable reflectors, along with the core barrel, were modeled as an integral structure during the initial optimization step. With the addition of the new coolant flow path, this heat structure

has three hydrodynamic volumes associated with it. The bypass through the outer reflector (volume 145) and the new coolant flow through permanent side reflector (volume 132) are modeled as the left and right volumes, respectively. As discussed earlier, the old coolant inlet flow (volume 130) was considered as a stagnant volume in the modified nodalization and was modeled as an adiabatic volume in the revised ATHENA model. This approximation, however, was used only for the initial optimization of pressure drop, amount of graphite removal, and the inlet flow velocity. This approximation gave conservatively higher vessel temperatures than would be expected with a more detailed analysis. To calculate vessel temperature precisely, this heat structure was split before the final detailed analysis was performed.

Fig. 6 shows the location of new coolant holes in the reflector region and the detailed ATHENA heat

structure model for the outer replaceable reflector, the permanent side reflector, and the reactor core barrel. The new ATHENA model has two heat structures for the reflector and core barrel with their interface at the centerline of the new coolant flow passages. The left heat structure, shown in Fig. 6, represents the replaceable outer reflector and about half of the PSR. The right heat structure represents the remaining outer portion of the PSR and the core barrel. Heat transfer from the inlet coolant flow in this revised model occurs at the interface between the two heat structures (i.e., between the right boundary of the left heat structure and the left boundary of the right heat structure). In the ATHENA model, this interface is at 19.05 cm from the inner face of the core barrel as shown in Fig. 6. To calculate the volumetric heat capacity of the graphite structure in PSR correctly, the coolant holes are considered as homogenized throughout the PSR. The density of graphite in the PSR is therefore reduced to account for the amount of graphite removed from the PSR to accommodate the coolant holes.

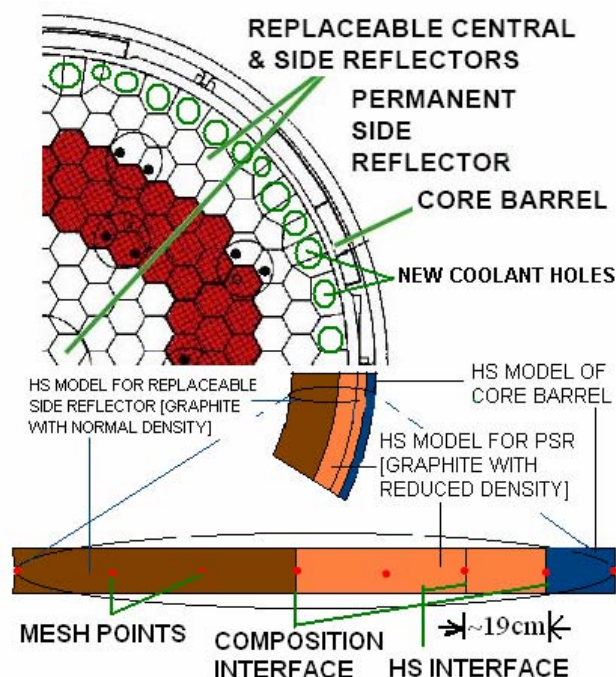


Fig. 6. Location of new coolant holes and heat structure model for reflector and core barrel

This modeling approach allowed an accurate representation of the new coolant flow path through the

outer reflector with minimal impact on the existing ATHENA models of the core and internal structures.

Conduction heat transfer was calculated for the new ATHENA model using the gap conductance for conduction enclosures. The gap conductance was computed as the thermal conductivity divided by the appropriate length. For axial conduction the axial distance between the heat structure's centers and for radial conduction the spacing between the adjacent structures are used as the length. View factors for conduction calculation were calculated and conservation of energy was evaluated using the reciprocity rule⁸.

VI. RESULTS & DISCUSSION

VI.A. Steady State Analysis

1. Coolant Temperature and its Influence on Different Reactor Parameters

To assess the impact of higher coolant temperatures on vessel temperatures with the current inlet flow configuration (through the peripheral channel boxes), sensitivity calculations were performed with varying coolant inlet and outlet temperatures. Table III shows the impact of changes in the coolant inlet and outlet temperatures on various steady-state reactor operating parameters. Case 1 shows the calculated steady-state operating parameters for the base case with nominal coolant inlet and outlet temperatures of 490 °C and 850 °C, respectively. Case 2 was a hypothetical case where the inlet temperature was unchanged, but the outlet temperature was increased from 850 °C to 950 °C. In this case, the coolant flow rate and the core pressure drop are decreased and the peak fuel temperature is increased significantly, but the vessel peak temperature and the heat rejected through RCCS were almost unchanged. In case 3, when both the coolant inlet and outlet temperatures were increased to 590 °C and 950 °C respectively, the calculated coolant flow rate and pressure drop closely matched the base case conditions, but the maximum vessel temperature and heat loss to the RCCS increased significantly. These results show the strong dependence of vessel temperatures on coolant inlet temperature for the current channel box coolant configuration.

2. Optimization of pressure drop, coolant velocity and the amount of graphite removal

Results from the optimization of the new flow configuration through the PSR are summarized in Table IV. This optimization involved a tradeoff between the

amount of graphite removed from the outer reflector and the pressure drop and velocities in the coolant flow channels through PSR. If too much graphite is removed there will be increased neutron leakage, resulting in less margin on reactivity control and higher neutron dose to the reactor vessel. If too little graphite is removed, the smaller flow area will lead to larger coolant pressure drops and

higher velocities in the PSR flow channels. The higher pressure drops reduce overall system efficiency, and the increased velocities can lead to significant differences between PSR inlet and core coolant velocities, which in turn, could result in increased lateral pressure gradient between the core and reflector and the increased potential for flow-induced vibration and cross-flow.

TABLE III
Increased inlet/outlet temperature and their effect on reactor parameters

Case	Coolant Inlet Temp (°C)	Coolant Outlet Temp (°C)	Coolant Flow Rate (kg/s)	Inlet Pressure (MPa)	Total Core Pressure Drop (kPa)	Maximum Fuel Temp (°C)	Maximum Vessel Temp (°C)	Heat Loss to RCCS (MW)	Core max velocity (m/s)
1	490	850	324	7.0	50.8	1009	453	3.29	49.0
2	490	950	253	7.0	33.86	1144	451	3.25	41.9
3	590	950	323	7.0	56.0	1106	541	4.49	53.0

TABLE IV
Optimization of flow area, inlet velocity and pressure drop

Case Number	Total Flow Area for Inlet Coolant (m ²)	Graphite from Outer Reflector Reduced by (%)	Number of Holes	Hydraulic Diameter (m)	Total Pressure Drop (kPa)	Steady State Fuel Temp (°C)	Steady State Vessel Temp < (°C)	Heat Loss to RCCS (MW)	Max Core Velocity (m/s)	Inlet velocity (m/s)
1	2.30965	14.13	36	0.2858	57.87	1106.07	454.1	2.517	53.20	34.83
2	2.285085	13.98	30	0.31142	57.80	1106.07	453.9	2.515	53.2	35.2
3			24	0.3482	57.67	1106.08	453.6	2.511	53.2	35.2
4			18	0.40204	57.52	1106.08	453.2	2.506	53.2	35.2
5	1.52339	9.32	24	0.3482	60.52	1106.08	453.7	2.514	53.215	52.81
6			18	0.3283	60.11	1106.08	453.5	2.510	53.21	52.81
7			12	0.40204	59.65	1106.09	452.8	2.503	53.21	52.81
8	1.14254	6.99	24	0.2462	64.93	1106.09	453.8	2.517	53.24	70.43
9			18	0.2843	64.09	1106.09	453.4	2.513	53.23	70.42
10			12	0.3482	63.12	1106.1	452.8	2.509	53.23	70.42
11	0.57127	3.495	24	0.1741	101.95	1106.11	453.5	2.509	53.47	141.1
12			18	0.201	97.03	1106.13	453.2	2.505	53.43	141.1
13			12	0.2462	91.41	1106.16	452.2	2.5	53.38	141.0

To minimize the amount of graphite removed from PSR, the cross sectional flow areas in the optimization of new inlet configuration were made less than the total inlet cross sectional area in the original ATHENA model for the channel box configuration (4.6193 m^2). As shown in Table IV, the total coolant inlet flow area for Case 1 was taken as 2.30965 m^2 which is half of the inlet flow area in the original ATHENA model. For Cases 2-4, the total flow area was assumed to be equal to the total flow area through the reactor core including the bypass flows. For these cases, the total flow area and the amount of graphite removed were constant, but the number of holes and their dimensions were changed. For Cases 5-7, 8-10 and 11-13, total flow areas were taken as 66.67%, 50% and 25% of total flow area through the reactor core.

Our focus during this investigation was on a number of parameters. The graphite removed from outer reflector to create the new coolant flow path has to be less than 20% of the total graphite in the outer reflector as recommended by GA. Column 3 in the above table shows the percentage of graphite removed from the outer reflector for each case. Column 6 shows the total vessel pressure drop for each case which is the sum of the inlet pressure drop and the reactor core pressure drop. Out of this total pressure drop, $\sim 55 \text{ kPa}$ pressure drop occurs within the core and the rest occurs within the inlet flow path through the reflector region.

From Cases 2-4, 5-7 and 8-10 of Table IV, it can be concluded that for a constant total inlet flow area, changing the number of holes results in a change in pressure drop which is caused by the change in hydraulic diameter of the coolant flow path. In addition, a change in total inlet flow area (by changing the amount of graphite removed) has a much larger impact on pressure drop.

For Cases 11-13, the fractional coolant pressure drop through outer reflector is high compared to Case 1-10. As a result the total pressure drop is more sensitive to the change in the hydraulic diameter of the inlet flow path through the reflector region.

As noted earlier, the total pressure drop through the reactor vessel is critical because a higher pressure drop requires higher pumping power, which directly affects the overall plant efficiency. In our case, it was decided to limit

the total reactor vessel pressure drop (column 6 of Table IV) to $\sim 90 \text{ kPa}$ which limits the required pumping power to about 3% of the total core thermal power. This pumping power is reasonable for the MHR and is less than the pumping power of a typical PWR ($\sim 5\%$). As discussed earlier, we also wanted to maintain the coolant velocity in the reflector region (column 11 in Table IV) close to the coolant velocity through the reactor core (column 10). These criteria lead to the optimized final coolant flow configuration described in the next section.

3. Final optimized coolant configuration

Considering all limiting criteria it can be concluded from Table IV that, with removal of about 10% of the graphite from the outer reflector (which gives a coolant flow area of $\sim 1.64 \text{ m}^2$), the inlet coolant velocity in the PSR is approximately equal to that in the core and a reasonable total pressure drop ($\sim 60 \text{ kPa}$) is obtained.

Based on the above criteria, the final design parameters developed for the coolant flow path through the outer reflector region are summarized in Table V. Considering the available thickness of the PSR and the space required for boronated rods, holes for coolant flow were selected with diameters of 10.16, 15.24 and 20.32 cm.

The steady-state operating conditions calculated by ATHENA, which are also summarized in Table V, appear to be reasonable. Core and PSR coolant velocities also appear to be consistent with each other. The steady-state reactor vessel temperature for a coolant inlet and outlet temperature of 590°C and 950°C , respectively, is 420°C , which is even less than the steady state vessel temperature of 451°C for the current MHR design with inlet and outlet temperatures of 490°C and 850°C , respectively. For this low reactor vessel temperature, the power loss through RCCS is less than the current design. Due to smaller equivalent hydraulic diameter, the total pressure drop for the final optimized coolant configuration was higher (80.2 kPa) than the initial optimization ($\sim 60 \text{ kPa}$). This pressure drop is within our limit (i.e. $< 90 \text{ kPa}$) and seems to be reasonable.

TABLE V
Final optimized coolant flow configuration

Total Flow Area for Inlet Coolant (m ²)	Graphite from Outer Reflector Reduced by (%)	Number of Holes and their diameter			Equivalent Hydraulic Diameter (m)	Total Pressure Drop (kPa)	Steady State Fuel Temp (°C)	Steady State Vessel Temp (°C)	Heat Loss to RCCS (MW)	Max Core Velocity (m/s)	Inlet velocity (m/s)
		10.16 cm	15.24 cm	20.32 cm							
1.6417	10.04	18	18	36	0.1651	80.2	1106	420	2.13	53.23	45.5

VI.B. Transient Analysis

The reactor vessel peak temperature response and the fuel peak temperature response for the revised coolant configuration were evaluated for both high pressure conduction cooldown (HPCC) and low pressure conduction cooldown (LPCC) events. For both cases the reactor is scrammed at the beginning of the transient. The initial conditions for these transient cases were taken from the steady state operating condition. The LPCC calculation assumed a rapid depressurization of the reactor primary system from the steady-state operating pressure to atmosphere conditions in about 50s. The HPCC calculation assumed a gradual depressurization of primary system pressure to about 5 MPa over a period of about 50 hours.

Peak reactor vessel temperatures for these calculations are shown in Fig. 7, and peak fuel temperatures are shown in Fig. 8. Since the pressurized helium in the high pressure scenario helps to remove heat by natural circulation, the peak fuel and reactor vessel temperatures both occur in the low-pressure transient. The peak fuel temperature of 1525 °C for the LPCC calculation occurred at approximately 60 hours after the transient was initiated, and the peak fuel temperature of 1349 °C for the HPCC calculation occurred at approximately 50 hours after transient initiation. In both cases, the calculated fuel temperature was below the design fuel temperature limit of 1600 °C.

The calculated peak reactor vessel temperatures shown in Fig. 7 were 517 °C for the LPCC calculation and 478 °C for the HPCC calculation, and occurred at approximately 70 hours after transient initiation in both cases. All of these transient results appear to be consistent with transient calculations performed earlier for the base case model without modifications to the coolant inlet flow configuration.

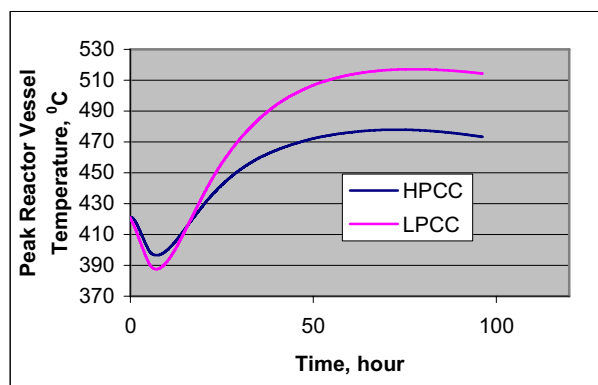


Fig.7. Peak reactor vessel temperature for pressurized and depressurized conduction cooldown

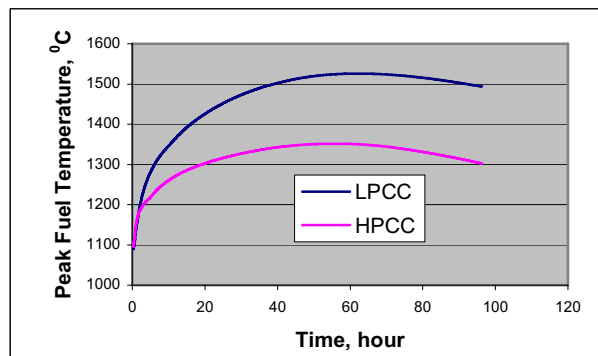


Fig. 8. Peak fuel temperature for pressurized and depressurized conduction cooldown

VII. CONCLUSIONS

An evaluation of an alternative configuration for the coolant inlet flow through the outer reflector region of the MHR was completed. With the removal of about 10% of the graphite from outer reflector (which corresponds to about a 5% reduction of the total graphite heat capacity in the entire core) for this new configuration, the vessel temperatures during steady state and transient operating conditions were found to be within the ASME code limits for the vessel material. For inlet and outlet temperatures of 590 °C and 950 °C, respectively, the steady state vessel temperature was found to be 541 °C with the original coolant inlet configuration. With the new alternative coolant flow configuration, the reactor vessel temperature was reduced to 420 °C. This reduced steady state reactor vessel temperature allows the MHR to operate at the higher coolant outlet temperatures required for efficient hydrogen production, and could result in a significant reduction in the cost of the reactor vessel material.

ACKNOWLEDGEMENTS

This work was funded in part by the US Department of Energy Nuclear Energy Research Initiative, under grant DE-FG03-02SF22609/A000.

NOMENCLATURE

ASME - American Society of Mechanical Engineers
GA - General Atomics
GT-MHR - General Atomics-Modular Helium Reactor
HS - Heat Structure
HTE - High Temperature Electrolysis
HPCC - High Pressure Conduction Cooldown
INL - Idaho National Laboratory
LPCC - Low Pressure Conduction Cooldown
MHR - Modular Helium Reactor
PSR - Permanent Side Reflector
RCCS - Reactor Cavity Cooling System
SI - Sulfur-Iodine

REFERENCES

1. ALBERT C. MARSHAL, *An Assessment of Reactor Types for Thermo Chemical Hydrogen Production*, SAND2002-0513, Sandia National Laboratory, (2002).
2. GENERAL ATOMICS, *Gas Turbine-Modular Helium Reactor (GT-MHR) Conceptual Design Report*, GA Document-910720, General Atomics, San Diego, CA, (1996).
3. PHILIP E. MACDONALD, et al., *NGNP Preliminary Point Design-Results of the Initial Neutronics and Thermal-Hydraulic Assessment*, INEEL/EXT-03-00870, Idaho National Laboratory, Idaho Falls, ID, (2003).
4. EDWIN HARVEGO, et al., "Hydrogen Production using the Modular Helium Reactor", *Proc. of the 13th International Conference on Nuclear Engineering*, ICONE13-50281, Beijing, China, (2005).
5. L. C. BROWN, et al, *High Efficiency Generation of Hydrogen Fuels Using Nuclear Power*, GA-A24285, General Atomics, San Diego, CA, (2003).
6. NATIONAL ACADEMY OF SCIENCE, NATIONAL RESEARCH COUNCIL, "The Hydrogen Economy: Opportunities, Costs, Barriers and R&D Needs", NRC Report, Washington DC, (2004).
7. MATT RICHARD, et al., "The H2-MHR: Nuclear Hydrogen Production Using the Modular Helium Reactor", *Proc. of the ICAPP 2005*, 5355, Seoul, Korea, (2005).
8. RELAP5-3D/ATHENA[®] Code Manual, Vol. I-V, Idaho National Laboratory, Idaho Falls, (2005).
9. RELAP-3D[®] Code Manual, Vol. I-V, Idaho National Laboratory, Idaho Falls, (1999).